1986

A Study on Starting Characteristics of a Rolling Piston Type Rotary Compressor

T. Yanagisawa

T. Shimizu

T. Horioka

A STUDY ON STARTING CHARACTERISTICS OF A ROLLING PISTON TYPE ROTARY COMPRESSOR

Tadashi Yanagisawa[1], Takashi Shimizu[1] & Tatsuya Horioka[1]

[1]Department of Energy and Mechanical Engineering, Shizuoka University, 3-5-1, Johoku, Hamamatsu, 432, JAPAN

ABSTRACT

The starting performance of a refrigerating compressor is as important as the steady performance of the compressor. This paper analyses the starting load torque of a rolling piston type rotary compressor theoretically and experimentally. The load torque is classified into the moments based on the vane spring force, the frictional moment at the thrust, the frictional moments at journal bearings. Theoretical results calculated using empirical coefficients of friction and the measured magnetic pull force are in good correlation with the experimental results. To control the starting load torque, it is suggested that the compressor should be assembled taking account of characteristics of the magnetic pull force of the motor.

INTRODUCTION

The starting performance of a refrigerating compressor is as important as the steady performance of the compressor. In the case of a rotary compressor, the starting performance depends not only on the design technique but also on the manufacturing technique. It has been reported that the starting load torque changes with the surface treatment of moving parts, the magnetic pull force of a motor and the interaction of refrigerating oil and refrigerant[1]. To assure the compressor to start smoothly, the motor is usually designed to have a fairly large starting torque estimated empirically, which sacrifices the steady performance of the motor and requires high-grade electrical parts.

Inspite of the importance of the starting characteristics of refrigerating compressors, there have been only a few reports[1] on them. In this paper, the load torque to start a rolling piston type rotary compressor is classified into basic components and they are analysed thoeretically and experimentally. Measures to control the starting load torque in manufacturing the compressor are suggested.

ANALYSES OF STARTING LOAD TORQUE

Structure of Compressor and Load Moment

Fig. 1 shows a schematic view of a rolling piston type rotary compressor used to study. A compression mechanism and a driving motor are set in a hermetic shell and they are combined by a shaft. Both ends of a cylinder are sealed by surfaces of main and subbearings which support the shaft. In the cylinder a rolling piston is mounted on an eccentric of the shaft and a vane loaded by a spring divides the crescent-shaped room into suction and compression chambers. The weight of the shaft and the motor rotor is supported by a thrust end of the shaft. The compression mechanism is submerged in refrigerating oil stored in the bottom of the shell.

When the compressor begins to start, the following load moments act on the shaft.
(1)Moments of forces acting on the eccentric of the shaft due to the vane spring force.
(2)Moments of frictional forces acting on contact points between the shaft and the bearings.
(3)A moment of the frictional force acting on the thrust of the shaft.
Other moments based on the viscosity of the oil are neglected and the pressure in the compressor is assumed to be balanced. The moment of inertia of the shaft is not important when the compressor begins to start very slowly.

Moments Based on the Vane Spring Force

As shown in Fig. 2, such forces as a spring force F_S, a normal contact force F_V and its frictional force $\mu_V F_V$ on the vane tip, normal contact forces R_{V1}, R_{V2} and their frictional forces $\mu_S R_{V1}$, $\mu_S R_{V2}$ on the vane sides, a normal contact force F_P and its frictional force $\mu_P F_P$ on the eccentric are assumed to act in the cylinder. The spring force F_S is put down as follows.

$$F_s = k(x_0 - x) \quad \cdots\cdots(1)$$

Where x:displacement of vane $\{=r_C+r_V-(r_P+r_V)\cos\alpha-e\cos\theta_S\}$, θ_S:angle of shaft, x_0:maximum deflection of spring, k:spring constant, r_C, r_P, r_V:radii of cylinder, rolling

piston and vane tip, $e=r_c-r_p$, $\alpha=\mathrm{Sin}^{-1}\{e\sin\theta_s/(r_p+r_v)\}$. The normal contact force F_v on the vane tip is derived from balancing equations of forces and moments[2].

$$F_v=F_s/\{\cos\alpha+\mu_v\sin\alpha+(\mu_s/a)|\Phi|\} \quad \cdots\cdots\cdots\cdots\cdots\cdots\cdots\cdots\cdots\cdots (2)$$

Where $\Phi=(\mu_v\cos\alpha-\sin\alpha)(a+2x-2r_v+b\mu_s)+2\mu_v r_v$,

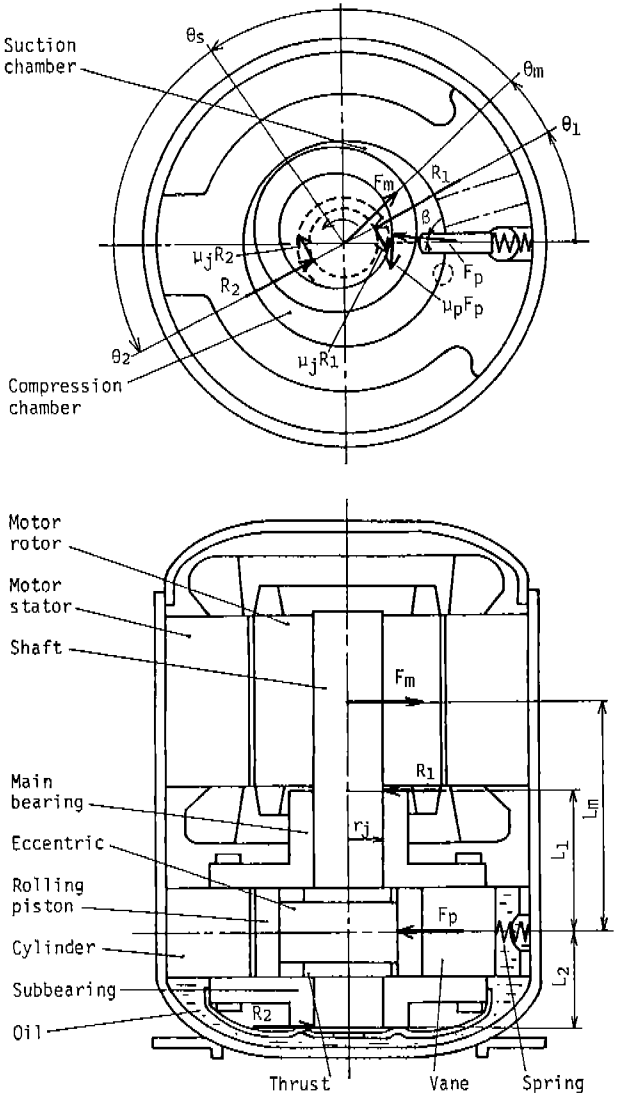

Fig. 1 A schematic view of a rolling piston type rotary compressor

a:length of vane slot, b:width of vane, μ_v,μ_s:coefficients of friction at vane tip and vane side.
On the rolling piston, balancing equations of moments and forces are expressed as follows.

$$\left.\begin{aligned} &r_p\mu_v F_v = r_e\mu_p F_p \\ &F_v = \mu_p F_p \sin(\beta-\alpha) + F_p\cos(\beta-\alpha) \\ &\mu_v F_v = \mu_p F_p \cos(\beta-\alpha) - F_p \sin(\beta-\alpha) \end{aligned}\right\} \quad \cdots\cdots (3)$$

Where r_e:radius of eccentric, μ_p:coefficient of friction at eccentric, β:angle of force F_p.
Rearranging Eq. (3), μ_v, F_p and β are derived respectively.

$$\mu_v = \mu_p / \sqrt{(1+\mu_p^2)(r_p/r_e)^2 - \mu_p^2} \quad \cdots\cdots (4)$$

$$F_p = (r_p\mu_v F_v)/(r_e\mu_p) \quad \cdots\cdots (5)$$

$$\beta = \alpha + \mathrm{Sin}^{-1}\frac{r_e\mu_p(\mu_p-\mu_v)}{r_p\mu_v(1+\mu_p^2)} \quad \cdots\cdots (6)$$

Based on the F_p and its frictional force $\mu_p F_p$, the following moments M_p and $M_{\mu p}$ act on the shaft.

$$M_p = -eF_p\sin(\theta_s+\beta) \quad \cdots\cdots (7)$$

$$M_{\mu p} = \mu_p F_p\{r_e + e\cos(\theta_s+\beta)\} \quad \cdots\cdots (8)$$

Empirical values are used for coefficients of friction.

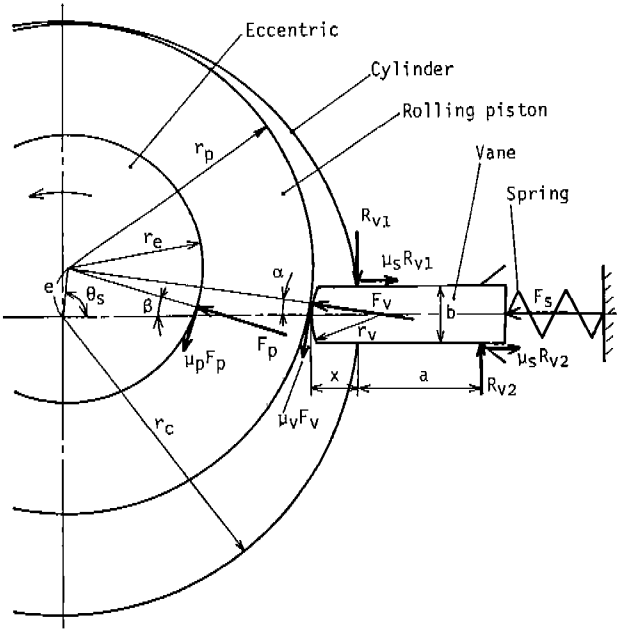

Fig. 2 Forces acting in the cylinder

Moments of Frictional Forces on Journal Bearings

Reaction forces on main and subbearings support the shaft against the vane spring force and their frictional forces cause load moments on the shaft. If the motor is accidentally assembled with an unbalanced air gap, the unbalanced magnetic pull force arises[3] and influences the reaction and frictional forces on the shaft. As shown in Fig. 1, under the condition that a normal force F_p and its frictional force $\mu_p F_p$ on the eccentric due to the spring force, a magnetic pull force F_m, reaction forces R_1, R_2 and their frictional forces $\mu_j R_1$, $\mu_j R_2$ act on the shaft, balancing equations of moments around the lower end of the shaft are put down as follows.

$$\left.\begin{aligned}(R_1\cos\theta_1-\mu_j R_1\sin\theta_1)(L_1+L_2)&=(F_p\cos\beta+\mu_p F_p\sin\beta)L_2-F_m L_m\cos\theta_m\\(R_1\sin\theta_1+\mu_j R_1\cos\theta_1)(L_1+L_2)&=(\mu_p F_p\cos\beta-F_p\sin\beta)L_2-F_m L_m\sin\theta_m\end{aligned}\right\}\quad\cdots\cdots(9)$$

Where θ_m, θ_1 : angles of F_m and R_1, L_m, L_1, L_2 : distances of F_m, R_1 and R_2, μ_j : coefficient of friction at journal. This yields the reaction force R_1.

$$R_1=\sqrt{(F_pL_2)^2(1+\mu_p^2)+F_m^2(L_m+L_2)^2-2F_pF_mL_2(L_m+L_2)\Psi}\,/\,\{(L_1+L_2)\sqrt{1+\mu_j^2}\}\quad\cdots(10)$$

Where $\Psi=\cos(\theta_m+\beta)+\mu_p\sin(\theta_m+\beta)$.
The reaction force R_2 is derived similarly.

$$R_2=\sqrt{(F_pL_1)^2(1+\mu_p^2)+F_m^2(L_m-L_1)^2+2F_pF_mL_1(L_m-L_1)\Psi}\,/\,\{(L_1+L_2)\sqrt{1+\mu_j^2}\}\quad\cdots(11)$$

The load moments M_{r1} and M_{r2} caused by frictional forces $\mu_j R_1$ and $\mu_j R_2$ are expressed as follows.

$$M_{r1}=\mu_j R_1 r_j \quad\cdots\cdots(12)$$

$$M_{r2}=\mu_j R_2 r_j \quad\cdots\cdots(13)$$

Where r_j : radius of journal. Experimental values are used for coefficient of friction at the journal.

Moment on the Thrust Bearing

The thrust of the shaft supports the weight of the shaft and the rotor and the frictional force of the weight causes a load moment M_t on the shaft.

$$M_t=g\mu_t m_t r_t \quad\cdots\cdots(14)$$

Where r_t : radius of frictional force, m_t : mass of shaft and rotor, μ_t : coefficient of friction at thrust, g : acceleration of gravity.
The frictional force is assumed to act at the point on a radius r_t on thrust radii r_{t1}, r_{t2} in the direction of the magnetic pull force as shown in Fig. 3. If r_t is on the larger radius r_{t1} of the thrust, r_t is equal to r_{t1} and if not, it is evaluated as follows.

$$r_t=\sqrt{r_{t2}^2+e^2+2r_{t2}e\cos(\theta_s-\theta_m+\phi)}\quad\cdots\cdots(15)$$

Where $\phi=\mathrm{Sin}^{-1}\{e\sin(\theta_s-\theta_m)/r_{t2}\}$.

Starting Load Torque

The load torque T_s to start the compressor is expressed by the summation of each load moment.

$$T_s=M_p+M_{\mu p}+M_{r1}+M_{r2}+M_t \quad\cdots\cdots(16)$$

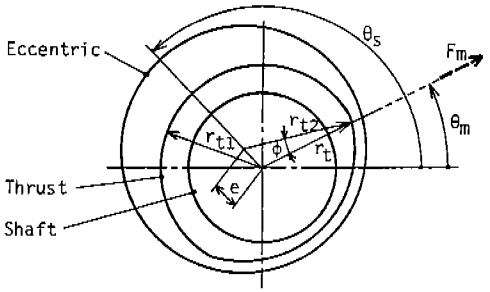

Fig. 3 Details of the thrust

EXPERIMENTS

Measurement of Coefficient of Friction

Coefficients of friction required to estimate the starting load torque are measured using practical parts smeared with refrigerating oil as lubricant. Fig. 4(a) shows an experimental apparatus to measure coefficient of friction between the shaft and the main bearing. The torque to begin rotating the shaft slowly is measured with a torque meter provided with a strain gauge. Considering balancing equations of forces and moments, the coefficient μ_j of friction is got as follows.

$$\mu_j = 1/\sqrt{(gmr_j(2l_2-l_1)/(Tl_1))^2-1} \quad \text{----------(17)}$$

Where m:mass of shaft and rotor, ℓ_1, ℓ_2:distances of reaction and load points.
The coefficient of friction between the shaft and the subbearing is measured similarly.

The load moment to begin rotating the shaft slowly on the thrust bearing is measured with the torque meter as shown in Fig. 4(b). The coefficient μ_t of friction is got as follows.

$$\mu_t = T/(gmr_t) \quad \text{----------(18)}$$

Where r_t:average radius of thrust, m:mass of shaft and rotor.

The force to begin rotating the rolling piston mounted on the eccentric is measured by pulling a string wound on the rolling piston as shown in Fig. 4(c). The coefficient μ_p of friction is got as follows.

$$\mu_p = r_p F/\sqrt{r_e^2(gm+F)^2-(r_p F)^2} \quad \text{----------(19)}$$

Where m:mass of rolling piston and weight.

Such coefficients of friction as μ_v at the vane tip and μ_s at the vane side are measured using the similar methods shown in Ref. (2).

Measurement of Unbalanced Magnetic Pull Force

The unbalanced magnetic pull force of a motor is measured at a static condition. Fig. 5(a) shows an experimental apparatus to investigate the direction of the force. A rotor is suspended with a string and a stator is set on a X-Y table to adjust the air gap. When the motor with the eccentric rotor is excited, the moving direction of the rotor is observed.

Fig. 5(b) shows an experimental apparatus to measure the unbalanced magnetic pull force. A stator is fixed to a base and a rotor can move on a guide rail. When the motor is excited, the pull force of the rotor is measured with a load cell and the displacement of the rotor is measured with a gap sensor. These outputs and

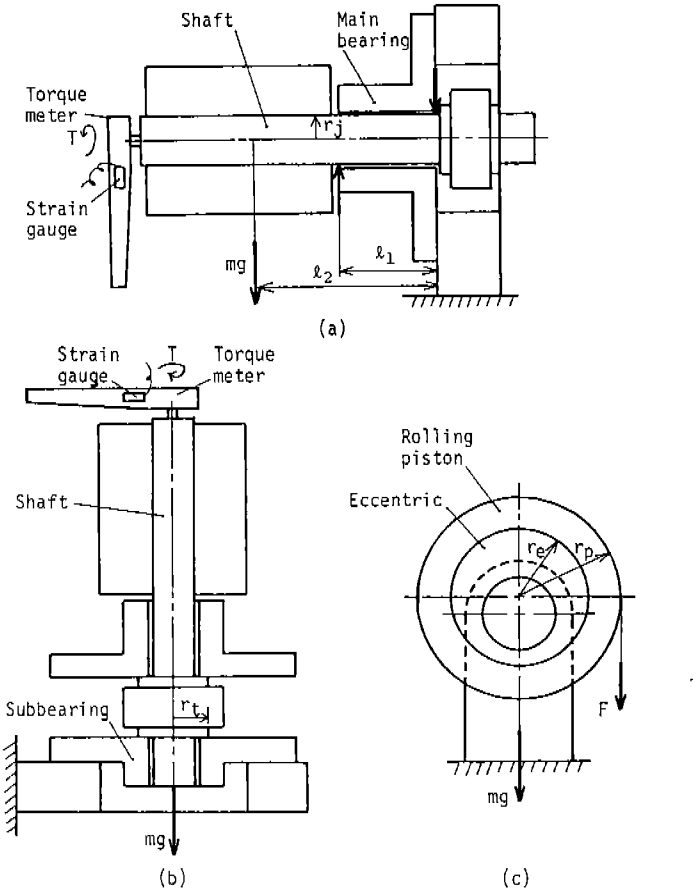

Fig. 4 Apparatus to measure coefficient of friction

the voltage of the exciting power are recorded on a ultraviolet oscillograph.

The motor used in experiments is a permanent split type 2 pole single phase induction motor and its nominal output is 750 W at 100 V, 60 Hz. The main winding and the auxiliary winding are located at right angles. The power reduced with a volt slider is supplied to the main winding and/or the auxiliary winding.

Measurement of Starting Load torque

Fig. 6 shows an experimental compressor to measure the starting load torque. At first, the torque to begin rotating the shaft slowly is measured with a torque meter under the condition that the pull force is loaded

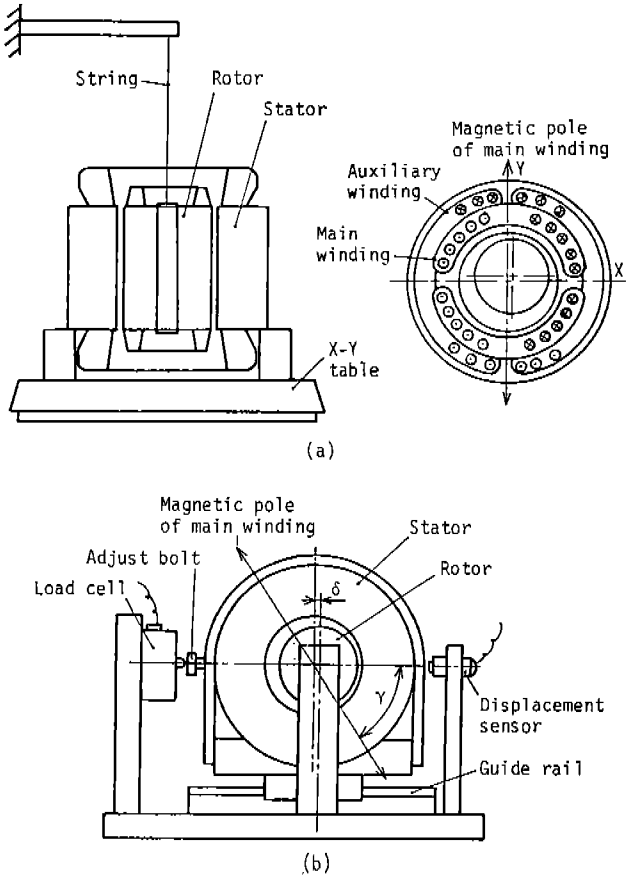

Fig. 5 Apparatus to measure the magnetic pull

at right angles to the shaft by a spring balance instead of the magnetic pull by the motor excitation. The output of the torque meter is recorded on a pen recorder. After removing the spring balance, the starting load torque is measured similarly under the condition that either the main winding or the auxiliary winding is excited. Experiments are executed in the atmosphere under the different conditions of the starting angle of the shaft, the pull force and its direction, the eccentricity of the motor and the exciting power. Table 1 shows main dimensions of the experimental compressor.

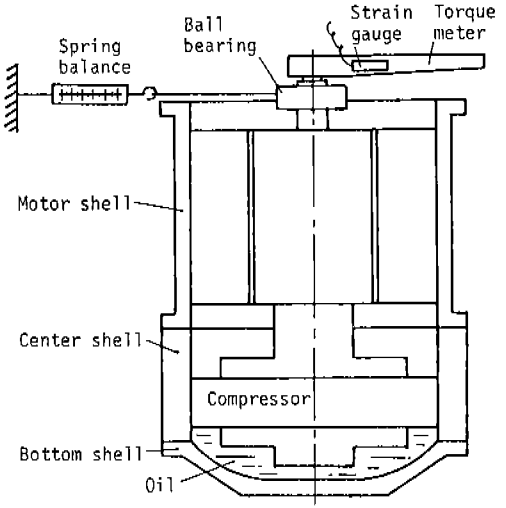

Fig. 6 Measurement of the starting load torque

Table 1 Main dimensions of the experimental compressor

Radius of cylinder	r_c	mm	27.0
Radius of rolling piston	r_p	mm	23.4
Radius of eccentric	r_e	mm	15.2
Radius of vane tip	r_v	mm	6.0
Radius of journal (shaft)	r_j	mm	9.6
Radius of thrust	r_{t1}	mm	13.4
Radius of thrust	r_{t2}	mm	14.4
Distance of pull force F_m	L_m	mm	96.9
Distance of reaction R_1	L_1	mm	51.9
Distance of reaction R_2	L_2	mm	29.4
Length of vane slot	a	mm	15.0
Width of vane	b	mm	4.7
Max. deflection of spring	x_0	mm	13.9
Spring constant	k	N/mm	1.36
Mass of shaft and rotor	m_t	kg	2.20

RESULTS AND DISCUSSIONS

Coefficient of Friction

Experimental results of coefficients of friction are listed in Table 2. Though the data have some scattering, typical values are used in principle in the calculation of the starting load torque. Concerning the value of μ_v at the vane tip, the measured value (=0.20) is larger than the value (=0.11) calculated from Eq. (4) using measured value (=0.17) of μ_p at the eccentric, which indicates that the rolling piston slides not on the vane tip but on the eccentric. The measured μ_p (=0.17) and the calculated μ_v (=0.11) are valid in the calculation of the load moment.

Unbalanced Magnetic Pull Force

When either the main or the auxiliary winding of the motor was excited in Fig. 3(a), the rotor was pulled in the direction perpendicular to the direction of magnetic poles of each winding. When both of the windings were excited, the rotor was pulled in the direction perpendicular to the direction of magnetic poles of the main winding. This is because the pull force by the main winding is much larger than that by the auxiliary winding.

Fig. 7 shows relationships between the magnetic pull force F_m, the eccentricity δ of the motor and the voltage E of the power. The force F_m increases almost in proportion to δ as shown in Fig. 7(a) and it increases paraborically with E as shown in Fig. 7(b).

Fig. 8 illustrates relationships between the pull force F_m and the direction angle γ of the eccentricity of the motor. F_m is obtained as the directional component of the measured pull force F_m' as shown in Fig. 8. Under the constant δ and E, F_m shows the maximum at $\gamma=90°$. Experimental results for the main winding are correlated as follows.

$$F_m=(8.24\times10^{-6}\gamma^2+0.056)\delta E^2 \quad \text{----------} \quad (20)$$

Here units are F_m [N], γ [°], δ [mm] and E [V]. These lines are illustrated in Figs. 7 and 8. Experimental

Table 2 Coefficients of friction

Coefficient of statical friction	Range of data	Typical value
μ_j at bearings	0.18~0.22	0.20
μ_t at thrust	0.16~0.20	0.18
μ_p at eccentric	0.16~0.18	0.17
μ_v at vane tip	0.18~0.22	0.20
μ_s at vane side	0.18~0.22	0.20

results for the auxiliary winding show the same tendency and are approximated as follows using the same units.

$$F_m = \{2.1\times10^{-7}(90-\gamma)^2+0.0004\}\delta E^2 \quad \cdots\cdots\cdots\cdots\cdots\cdots\cdots\cdots\cdots\cdots (21)$$

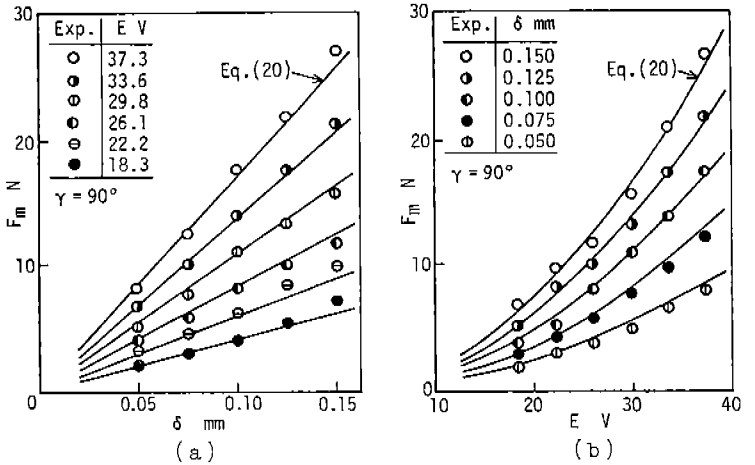

Fig. 7 Relationship between magnetic pull force, eccentricity and voltage

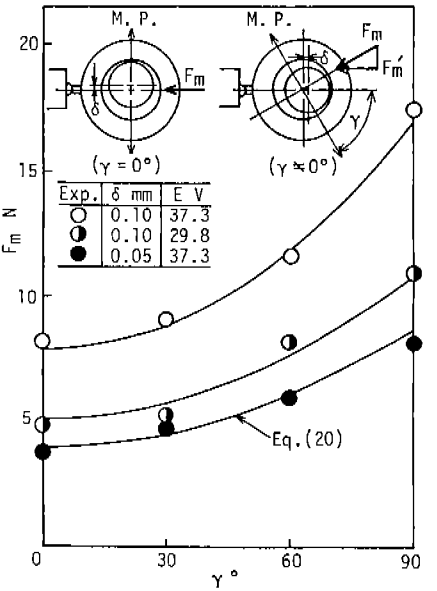

Fig. 8 Relationship between magnetic pull force and direction angle of eccentricity

The force of the auxiliay winding is much smaller than that of the main winding because of the less current. Practically the magnetic pull force of the motor at the starting can be estimated only by that of the main winding.

Starting Load Torque

Fig. 9 shows the change of the starting torque T_s measured under the condition that the pull force F_m of the spring balance acts on the shaft at L_m=188.8 mm and in the direction θ_m=0°. T_s changes with the starting angle θ_s of the shaft and it records the minimum at around θ_s=90° and the maximum after θ_s=270°. With the increase of F_m, T_s shifts positively but its amplitude hardly changes. This is because the amplitude of T_s depends on the force of the vane spring and the average of T_s depends on the reaction forces against the pull force. Theoretical lines calculated using empirical coefficients of friction are also illustrated by the solid lines in Fig. 9 and they are in good correlation to experimental data in the case of the smaller F_m. But in the case of the larger F_m, dotted lines calculated using the maximum value (=0.22) of the measured μ_j show better fitting to the measured data.

Components of the starting load torque are illustrated in Fig. 10 as the result of the theoretical calculation. The moment M_p based on the vane spring force changes like a inverse SIN curve against the starting angle θ_s of the shaft. The frictional moment

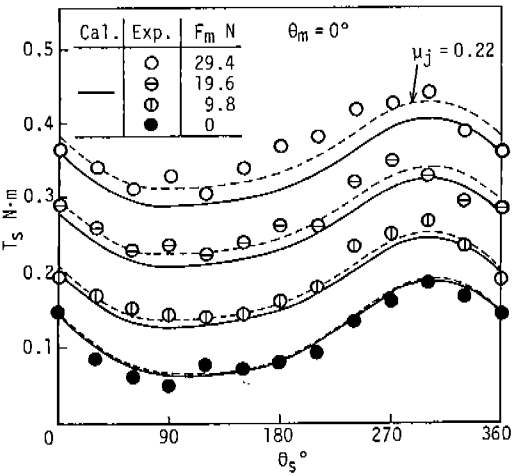

Fig. 9 Relationship between starting load torque ahd shaft angle (1)

$M_{\mu p}$ at the eccentric shows the minimum at θ_s=180° by the multiplication effect of changes of the spring force and the frictional radius. The frictional moment M_t at the thrust bearing and the frictional moments M_{r1}, M_{r2} at the journal bearings are almost constant. The later two increase greatly with the increase of the pull force F_m.

The starting load torque T_s changes with the direction θ_m of the pull force F_m as shown in Fig. 11. T_s in the case of θ_m=180° is less than that in the case of θ_m=0°. This is because reaction forces and their frictional forces at the journal bearing changes with

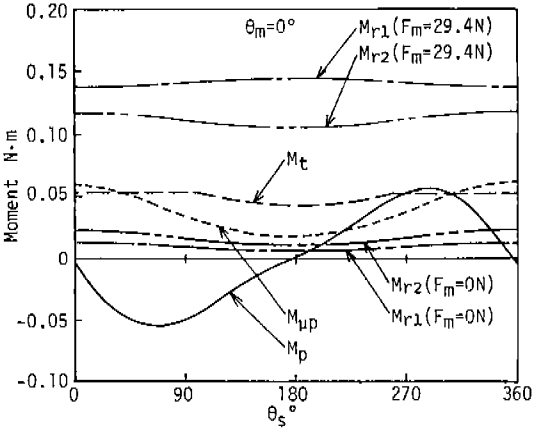

Fig. 10 Components of starting load torque

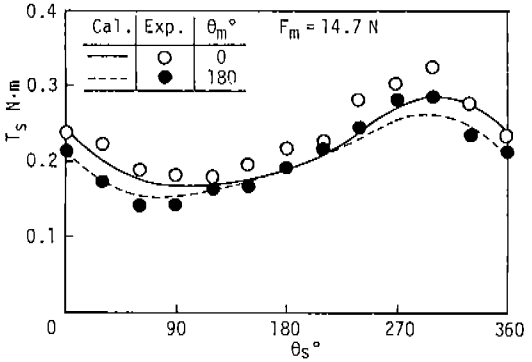

Fig. 11 Relationship between starting load torque and shaft angle (2)

the direction of the pull force and they are less in the case of θ_m=180°. This indicates that even if the same pull force acts, one in the direction against the vane direction is desirable to control the starting load torque.

Fig. 12 shows the change of T_s measured under the condition that the main winding is excited. The change of T_s against the starting angle θ_s is in the same manner as that shown in Fig. 11 where the pull force is loaded by the spring balance. The average of T_s changes with the direction γ of the motor eccentricity and T_s in the case of γ=30° is less than that in the case of γ=90°. This is because the magnetic pull force is less in the case of the smaller γ as shown in Fig. 8. Theoretical lines calculated from Eq. (16) using the magnetic pull force of Eq. (20) are in good correlation with experimental results.

If some eccentricity of the motor cannot be avoided in the assembly of the compressor, it is desirable to assemble the compressor in the way the direction of the motor eccentricity coinsides with the direction of magnetic poles of the main winding to control the starting load torque. As the compressor cylinder is usually inserted in the shell referring to its outer walls at the vane and anti-vane sides, it tends to incline in the direction perpendicular to the vane direction. To control the magnetic pull force of the motor and the starting load torque of the compressor, it is advisable to assemble the motor in the shell in the way the direction of magnetic poles of the main winding meets at right angles to the direction of the vane.

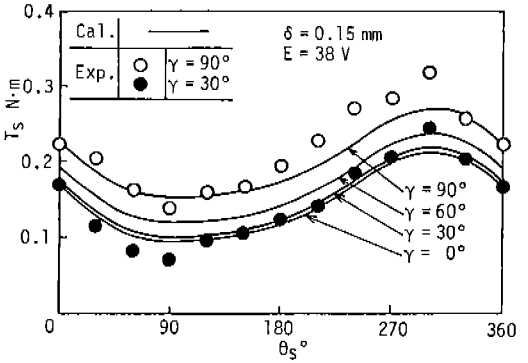

Fig. 12 Relationship between starting load torque and shaft angle (3)

Fig. 13 shows the influence of the contact ponts between the shaft and the bearings on the starting load torque T_s. Even if the pull force F_m is constant, T_s calculated theoretically differs by the contact way (1)∿(6) and it increases with the increase of the distance between the reaction points of R_1 and R_2. It is desirable that the shaft contacts with the upper end of the main bearing and the subbearing. The experimental results shown in Fig. 13 have the same tendency as that of the theoretical results.

CONCLUSIONS

In this paper, the starting load torque of a rolling piston type rotary compressor is classified into moments based on the vane spring force, the frictional force at the thrust and the frictional forces at the bearings. Theoretical results calculated using empirical coefficients of friction and the measured magnetic pull force are in good correlation with the experimental results. It is important to assemble the compressor taking account of the direction of the magnetic pull force of the motor.

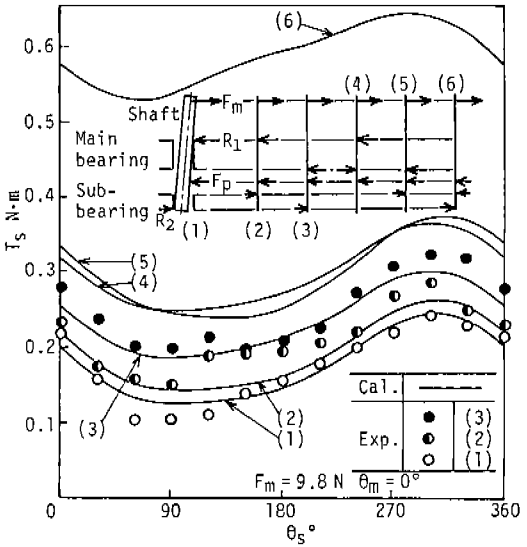

Fig. 13 Relationship between starting load torque and shaft angle (4)

ACKNOWLEDGEMENT

We are grateful to Mitsubishi Electric Corporation for providing experimental compressors.

REFERENCES

(1)Nagatomo, S. and Kato, S., Proc. Purdue Compressor Tech. Conf., (1980), 98.
(2)Yanagisawa, T., et al., Proc. Purdue Compressor Tech. Conf., (1982), 185.
(3)Covo, A., AIEE Trans., Dec. (1954), 1421.